Solar Cells Efficiency enhancement using multilevel Selective Energy Contacts (SECs)

Mohammad Eskandari
University of Tabriz
Azeez Barzinjy
Salahaddin University - Erbil College of Education
Ali Rostami (rostami@tabrizu.ac.ir)
University of Tabriz https://orcid.org/0000-0002-8727-4711
Ghasem Rostami
University of Tabriz
Mahboubeh Dolatyari
University of Tabriz

Research Article

Keywords: Hot Carrier Solar Cells, Energy Selective Contacts, Efficiency, Detailed Balance model, Entropy

Posted Date: August 11th, 2021

DOI: https://doi.org/10.21203/rs.3.rs-670558/v1

Version of Record: A version of this preprint was published at Optical and Quantum Electronics on January 4th, 2022. See the published version at https://doi.org/10.1007/s11082-021-03493-8.

Solar Cells Efficiency enhancement using multilevel Selective Energy Contacts (SECs)

M. Esgandari[1], Azeez A. Barzinjy[2, 3], A. Rostami[1, 4, 5], G. Rostami[5] and M. Dolatyari[5]

[1] OIC Research Group, University of Tabriz, Tabriz, 5166614761, Iran.
[2]Department of Physics, College of Education, Salahaddin University-Erbil, Iraq
[3]Physics Education Department, Education Faculty, Tishk International University, Erbil, Iraq
[4] Photonics and Nanocrystal Research Lab. (PNRL), Faculty of Electrical and Computer Engineering, University of Tabriz, Tabriz 5166614761, Iran.
[5] SP- EPT Labs, ASEPE Company, Industrial Park of Advanced Technologies, 5364196795, Tabriz, Iran
rostami@tabrizu.ac.ir

Abstract: High-energy coming photons can be absorbed and lead to generate hot carriers. In normal solar cells, these carriers are scattered, by electron-electron and electron-lattice mechanisms, and rapidly lose extra energy then approach the conduction band energy edge. This event in addition to other loss mechanisms causes the efficiency reduction in the solar cells to a limited value, theoretically 33%. Accordingly, the efficiency of solar cells can be enhanced considerably, if one makes the possibility for carriers that can be extracted rapidly before scattering and releasing extra energy to the lattice. This type of solar cell is called hot carrier solar cells (HCSCs). To this end, to improve the conversional efficiency, multilevel energy selective contacts (ESCs) as a new concept and new mechanism in solar cells can be utilized. In the other words, several appropriate energy levels as carrier extraction contacts in the conduction band are introduced. Here, we use multilevel ESCs, and based on our simulation it is shown that the maximum efficiency of 75% is achievable for low bandgap materials. For a typical material such as Si, the maximum efficiency is increased to 60% using ten ESCs.

Keywords: Hot Carrier Solar Cells; Energy Selective Contacts; Efficiency; Detailed Balance model; Entropy.

1. Introduction

In a conventional solar cell, thermalization losses of photo-generated carriers are an important issue that decreases conversional efficiency. Thermalization refers to the carriers that have excess energy higher than the bandgap of absorber materials. The absorbed carriers emit energy as a phonon to reach the band edge and release their energies as heat [1]. The effect of this phenomenon can be seen in the shortage of power conversional efficiency. So, if these carriers can be extracted rapidly, the efficiency will be increased and overcomes the Shockley- Queisser limit [2]. Shockley and Queisser showed that the maximum efficiency for single-junction solar cells is 40.7% that can be obtained for materials with a bandgap of 1.12 eV [3]. There are some ways to overcome this limitation such as introducing impurity levels [4-6], multi-junction, Multiple Exciton Generation (MEG) [7], and hot carrier extraction

before wasting their energies [8]. Intermediate Band Solar Cells (IBSCs) increase the efficiency using the absorption of the low energy photons in two or more steps (up-conversion), in addition to the valence band to conduction band transitions in traditional solar cells [9-11]. The multi-junction method splits the spectrum into several spectra and light is absorbed with well-matched absorbers such as tandem solar cells [12]. Another method is the hot carrier extracting related to the high-energy photons. It is an important mission to provide a method to decrease dissipation time and extracting the carriers immediately before their completely thermalizing. If the thermalizing time is assumed to be 1ns, then the conversional efficiency power will be higher than the efficiency related to the single-junction solar cells. Thus, the efficiency can be improved with increasing of this time. For extraction of hot carriers, energy selective contacts (ESCs) are purposed. ESCs, in turn, are double barrier resonant tunneling diodes consisting of Si quantum dots embedded in SiO_2 matrices [13].

In this investigation, the authors are introducing a new model to extract the hot carriers based on multiple ESCs implanted on the valance and conduction band. Fig. 1 shows the schematic diagram of the proposed model. The width of each ESC has been assumed to be zero and their intervals are $\Delta\varepsilon$.

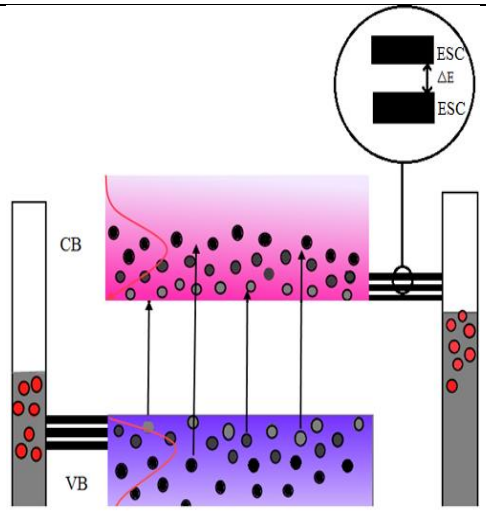

Fig. 1. Schematic diagram of multiple Energy Selective Contacts

2. Effect of Thermalization time on Hot Carrier Solar Cells

To analyze a hot carrier solar cell we make two assumptions: (i) an absorber with a bandgap that generates carriers with photoexcitation. (ii) Multiple Selective Energy Contacts (ESCs) implanted on the conduction band and valance band at each specific energy level that can extract hot carriers to metal electrodes [13]. Additionally, enough time requires for hot carriers to reach the electrodes. This time is called the thermalization time and here we assumed a finite thermalization time.

2.1. Detailed Balance model for particles and energy fluxes

To calculate the conversional efficiency of an HCSC, a detailed balance model for particles, energy fluxes, and entropy generation are considered. The output current (I_{out}) accounted for the difference between absorbed and emitted photon fluxes.

$$I_{out} = I_{abs} - I_{em} \tag{1}$$

$$I_{out} = qA\int_{\varepsilon_{cv}}^{\infty} \left(I_{sun}(\varepsilon) - I_{cell}(\varepsilon, \mu_{cv}, T_h)\right) d\varepsilon \tag{2}$$

Where, ε_{CV} is the difference between energy levels in the conduction and valance bands. T_h is the hot carrier temperature and I_{cell} is the emitted photon flux from the cell that is calculated from Plank's law [1].

$$I_{cell} = \frac{2\pi}{h^3 c^2} \frac{\varepsilon^2}{exp\left[(\varepsilon - \mu_{cv}) / K_B T_h\right] - 1} \tag{3}$$

Where h represents the Planck constant, c is the velocity of light; K_B is the Boltzmann constant and μ_{CV} is the chemical potential. Energy flux extracted from the cell is the balance of the absorbed energy, U_{abs}, and dissipated energy created by emitted energy, U_{em}, and thermalized energy, U_{th}, respectively [14,15].

$$U_{abs} = \int_{\varepsilon_{cv}}^{\infty} \varepsilon I_{cell}(\varepsilon, 0, T_{sun}) d\varepsilon \tag{4}$$

$$U_{em} = \int_{\varepsilon_{cv}}^{\infty} \varepsilon I_{cell}(\varepsilon, \mu_{cv}, T_h) d\varepsilon \tag{5}$$

$$U_{th} = 3K_B n\left(T_h - T_{RT}\right) d / \tau_{th} \tag{6}$$

In equation (6) d represents the thickness of the absorber and its value is assumed to be 500 nm [15], τ_{th} is the thermalization time, T_{RT} is the room temperature and n is the carrier density that accounted from equation (7).

$$n = \frac{8\sqrt{2}\pi m^{*3/2}}{h^3} \int_{\frac{\varepsilon_{cv}}{2}}^{\infty} \sqrt{\varepsilon - \varepsilon_{cv}/2} \frac{d\varepsilon}{\exp\left[\frac{\varepsilon - \mu_{CV}/2}{K_B T_h}\right] + 1} \tag{7}$$

In equation (7), m^* is the effective mass of electrons in the conduction band and the valance band. For numerical simulation m^* *is* $0.01m_0$ (m_0 is the rest mass of an electron). The energy extracted from the absorber by

one carrier is equal to the ratio of $\Delta\varepsilon$ and I_{out}/q, which is the difference between the ESC levels for electrons and holes ($\Delta\varepsilon$).

$$\Delta\varepsilon = \Delta U / \left(I_{out} / q\right) \tag{8}$$

For extracting hot carriers in T_h to electrodes at temperature T_{RT}, entropy should be generated [1, 15], and the output power could be calculated from:

$$p_{out} = \Delta U - T_{RT}\Delta S \tag{9}$$

In equation (9), $T_{RT}\Delta S$ can be written as:

$$T_{RT}\Delta S = \left(\Delta U - \left(I_{out}/q\right)\mu_{cv}\right)T_{RT}/T_h \tag{10}$$

And finally, the conversion efficiency (η) written as:

$$\eta = p_{out} / \int_0^\infty \varepsilon I_{sun}(\varepsilon)d\varepsilon \tag{11}$$

2.2. Effect of thermalization on efficiency

Fig. 2 shows the efficiency contrasted with the bandgap of the absorber in various thermalization times. The S-Q model for a single junction is shown in the black curve. The maximum efficiency of 40.7% is achievable for the material with a bandgap of 1.12 eV. Increasing the thermalization time to 1 ns shifts the maximum efficiency to the bandgap of 0.55 eV and the resultant efficiency is about 70% for this condition. Also, with a thermalization time of 100 ns, the maximum efficiency reaches 82% and the corresponding bandgap will be 0.5 eV.

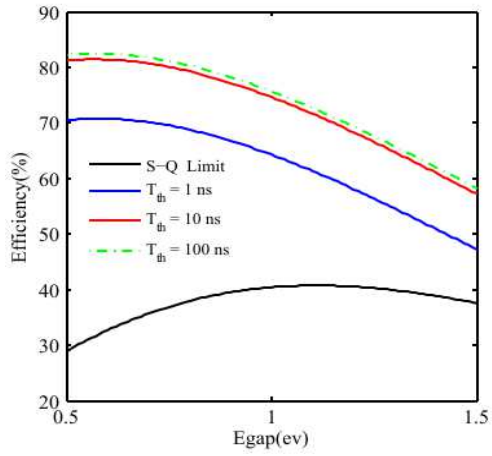

Fig. 2. Efficiency versus bandgap in various thermalization times

Fig. 3 (a) shows efficiency versus bandgap in various thermalization temperatures (T_H). When T_H is equal to 600 K, the efficiency reaches the upper than the S-Q limit (48%) and when T_H is 3600 K the efficiency reaches the maximum value. Fig. 3 (b) Shows that when T_H = 3500K, the efficiency is constant, and increasing the T_H more than this point does not affect the efficiency of the cell.

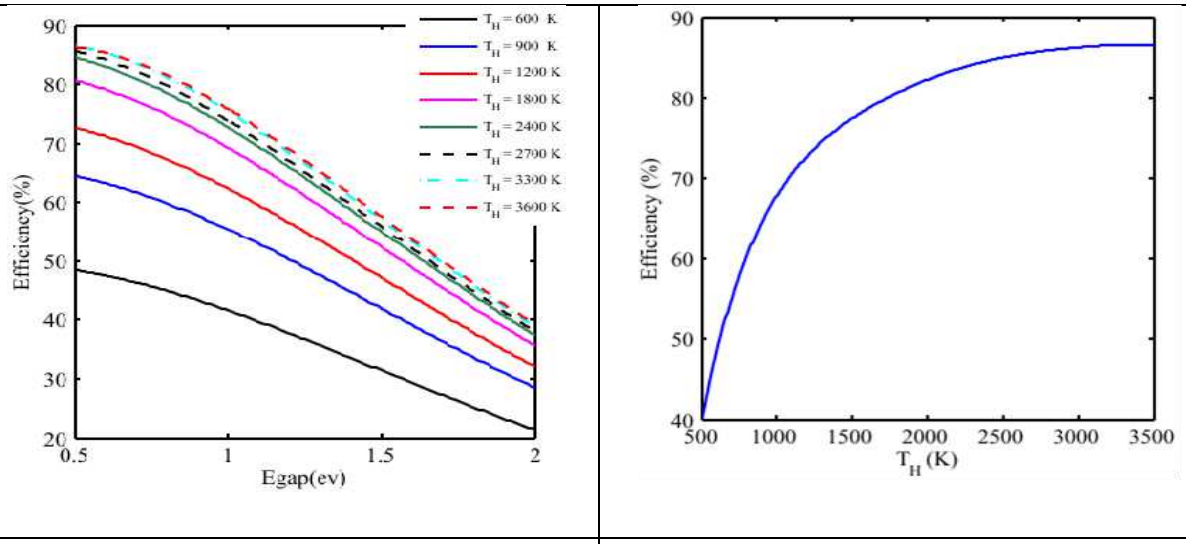

(a) **(b)**

Fig. 3. Efficiency versus (a) bandgap in different thermalization temperatures (b) thermalization temperatures

3. Multilevel Energy Selective Contacts (ESCs)

Fig. 1 shows multilevel Energy Selective Contacts for extracting hot carriers from different energy levels in conduction and valance bands. The width of ESCs is narrow to reduce the entropy generation in extracting hot carrier to cold electrodes [13]. For evaluating the performance of this type of hot carrier solar cells the detailed balance model is generalized and the output current density is written as:

$$J_{out} = q\left\{\sum_{i=1}^{n}\left[N\left(\varepsilon_l,\varepsilon_h,0,T_S\right)-N\left(\varepsilon_l,\varepsilon_h,\mu_l,T_C\right)\right]+N\left(\varepsilon_h,\infty,0,T_S\right)-N\left(\varepsilon_h,\infty,\mu_h,T_C\right)\right\} \quad (12)$$

$$\left(\varepsilon_l=\varepsilon_{cv}+2(i-1)\delta\varepsilon \quad , \quad \varepsilon_h=\varepsilon_{cv}+2i\delta\varepsilon\right)$$

In equation (12) *n* is the number of implanted ESCs and *N* is the particle flux and comes from plank's law [1].

$$N(\varepsilon_l,\varepsilon_h,\mu,T)=\frac{2\pi}{h^3C^2}\int_{\varepsilon_l}^{\varepsilon_h}\frac{\varepsilon^2 d\varepsilon}{\exp\left[(\varepsilon-\mu)/KT\right]-1} \quad (13)$$

The chemical potential of each ESC according to the difference between ESCs can be written as:

$$\mu_l = \left(\varepsilon_{fc} + (i-1)\delta\varepsilon\right) - \left(\varepsilon_{fv} - (i-1)\delta\varepsilon\right) \tag{14}$$

$$\mu_h = \left(\varepsilon_{fc} + i\delta\varepsilon\right) - \left(\varepsilon_{fv} - i\delta\varepsilon\right) \tag{15}$$

δε is the interval of ESCs in the valance and conduction bands. The output voltage from each ESC can be written as a function of the location of ESCs in valance and conduction bands:

$$V_{out}(i) = \left(\varepsilon_{CV} + 2i\delta\varepsilon\right)\left(1 - \frac{T_C}{T_S}\right) \tag{16}$$

Where, T_c and T_s are the cell and sun temperatures, respectively. The total output power is the sum of generated powers from each ESCs and power conversion efficiency is the ratio of output power to input power. The input power can be calculated from $p_{in} = \sigma T_s^4$, where σ is the Stephan-Boltzmann constant and is equal to $5.67 \times 10^{-8} W.m^{-2}.k^{-4}$ [16].

$$p_{out} = \sum_{i=1}^{n} J_{out}(i) \times V_{out}(i) \tag{17}$$

$$\eta = \frac{p_{out}}{p_{in}} \tag{18}$$

For evaluating the effect of the location of each ESC on the efficiency of the cell, the number of ESCs is considered as one, two, three, four, five, and ten. So the efficiency variations were plotted versus the location of ESCs. In the case of one ESC, the efficiency cannot increase and becomes lower than the S-Q limit (40.7%). This is due to that ESC is implanted in the edge of conduction and valance bands then swept to the upper energies in these bands. The location of ESC denotes the new bandgap for the absorber and new output voltage in sweeping is obtained while the current is decreased. For each level, while the output voltage is increased, the output current of the absorber decreases, and finally, the reduction of current prominent and the output power decreases. When we use one ESC (since a new bandgap for absorber is created) the S-Q limit reaches to lower value of bandgap as shown in Fig. 4 (a). In other words, when we use a low bandgap absorber, we expect that efficiency should be low, while by using ESC, efficiency reaches a maximum limit of S-Q. Another result from this achievement is removing the restriction for choosing the appropriate material to reach the high efficient solar cells.

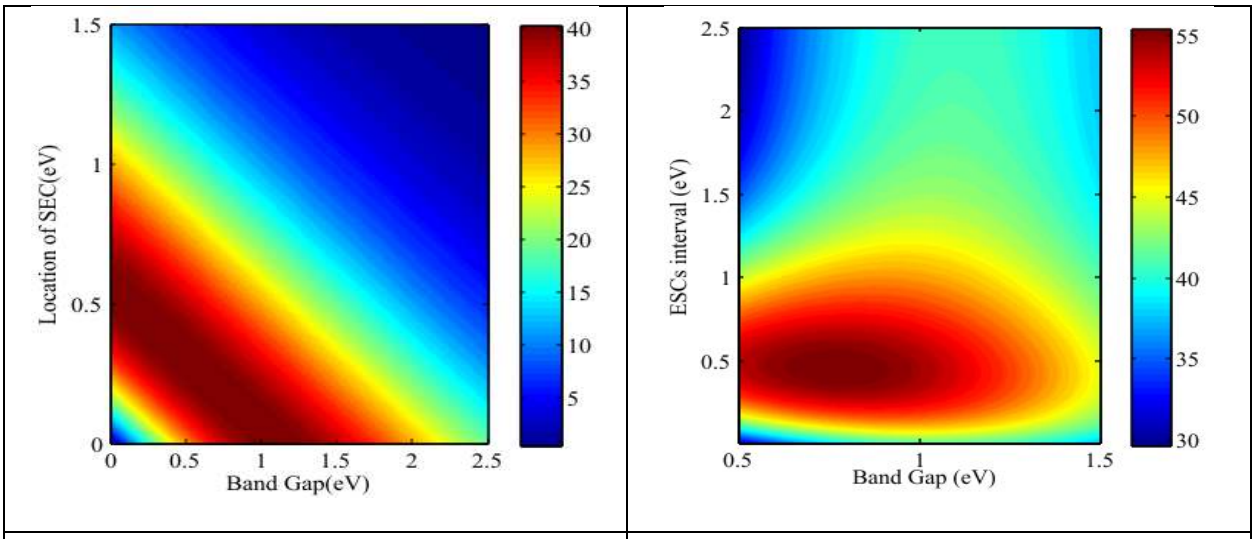

(a) **(b)**

Fig. 4. Efficiency versus the location of ESC in (a) one ESC and (b) two ESCs

Fig. 4 (b) shows the efficiency contour for two ESCs that are implanted symmetrically on the conduction and valance band. The dark region for materials with a bandgap of 0.7 eV to 0.9 eV and ESCs interval at 0.5 eV shows that the efficiency breaks the S-Q limit and is increased to 55%. In this case, the first ESC is implanted in the edge of the conduction and valance band and the second ESC with an interval of $\delta\varepsilon$ is upper than the first one and the extracted voltage from the absorber is more than one case. Fig. 5 shows efficiency contour plots for three, four, five, and ten ESCs which are implanted symmetrically on the conduction and valance bands. In Fig. 5 (a) the dark region indicates that maximum efficiency is about 63% for materials with band gaps between 0.4 eV to 0.8 eV and location of ESCs around 0.4 eV.

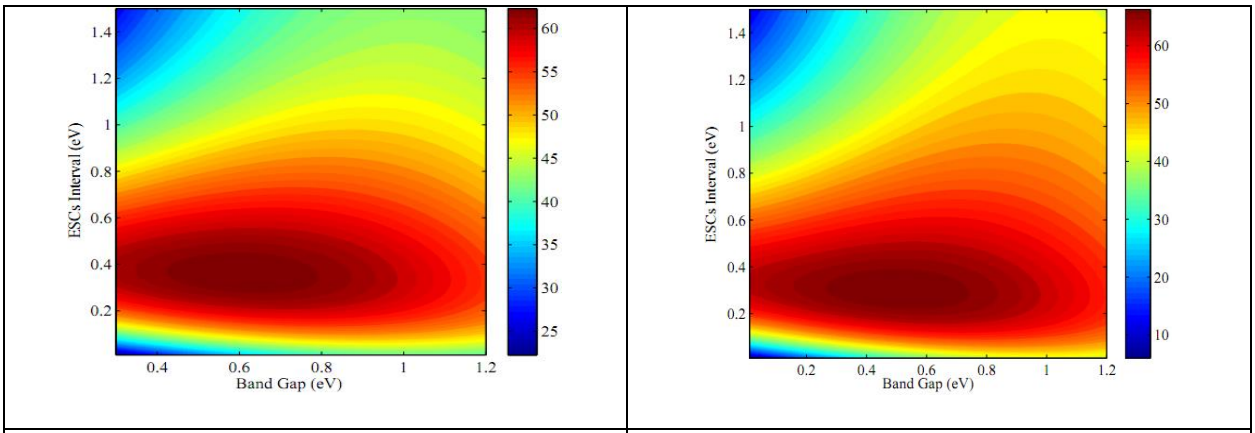

(a) **(b)**

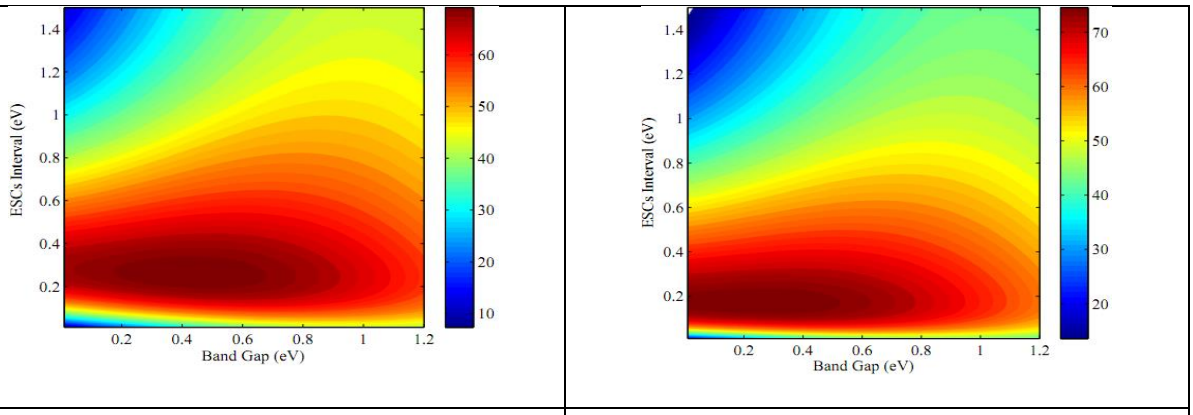

(c) **(d)**

Fig. 5. Efficiency versus the location of ESCs in (a) three cases (b) four cases (c) five cases (d) ten cases

To achieve higher efficiency, we use ten ESCs implanted on the conduction and valance bands symmetrically with δε intervals. Fig. 5 (d) shows that for materials with a bandgap between 0 eV to 0.5 eV and interval of ESCs around 0.2eV, the maximum efficiency is obtained as 75%. In this way, we decrease the thermalization of hot carriers by extracting them using the two, three, four, five, and ten ESCs. Using this method, the maximum efficiency is achievable for low bandgap materials too. In typical semiconductors, low bandgap materials create low output voltage with high output current and we need to have an optimum bandgap to reach the maximum efficiencies. This condition causes a restriction for choosing the best material for achieving high efficiencies. In our proposed model we can use zero bandgap materials (such as graphene) with ten ESCs while we have high power conversion efficiency.

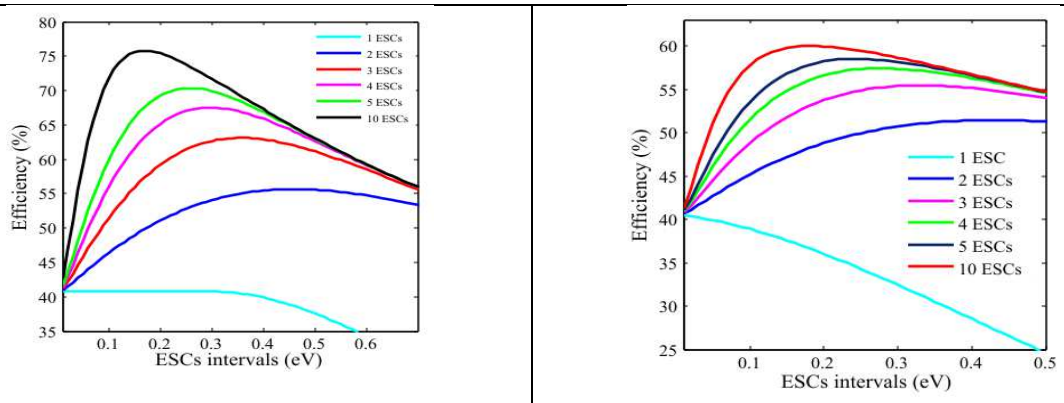

(a) **(b)**

Fig. 6. Efficiency versus Intervals ESCs in one, two, three, four, five, and ten ESCs implanted on the conduction and valance band symmetrically (a) different material (b) typical material (Si)

Fig. 6 (a) shows the effect of the number of ESCs on the efficiency which promoted to 75% using ten ESCs. In this case, we use one, two, three, four, five, and ten ESCs on the conduction and valance bands. The efficiency increases in all cases except one ESC case. This is, more likely, due to sweeping the location of ESC in upper energies which increases the effective bandgap of the material. The larger bandgap has a larger open-circuit voltage with a lower output current, and the current degrades the efficiency. When the number of ESCs is more than one, the S-Q limit is broken and the efficiency will reach 55%, 63%, 67%, 70%, and 75% for two, three, four, five, and ten ESCs respectively.

Fig. 6 (b) shows the efficiency versus the location of ESCs in a typical material like Si that indicates if we use more than one ESC we can achieve high efficiency and breaks the Shockley-Queiser limit for single-junction solar cells based on Si. In this type of solar cell, if ten ESCs are utilized then the efficiency increases and reach 60%.

4. Conclusions

In this study, ultra-high efficiency solar cells using minimizing the thermalization energy were demonstrated. To this end, multiple Energy Selective Contacts were used to allow the rapid collection of the hot carriers to contacts. Due to the fast carrier extraction process, we illustrated that the conversion efficiency of single-junction solar cells can be increased. We calculated the precise position of ESCs in the energy domain. The simulated results of this study showed that the efficiency of Si-based solar cells can be increased from 40.7% in classical case to 60% with applying ESCs by using ten ESCs.

5. References

1. M. A. Green. Third Generation photovoltaic: advanced solar energy conversion. Vol. **12**. Springer (2006).
2. W. Shockley, H. J. Queisser. “Detailed balance limit of efficiency of p-n junction solar cells”. *Journal of applied physics,* **32**(3), 510-519 (1961)
3. C. H. Henry. “Limiting efficiencies of ideal single and multiple energy gap terrestrial solar cells”. *Journal of applied physics*, **51**(8), 4494-4500 (1980).
4. M. J. Keevers and M. A. Green. “Efficiency improvements of silicon solar cells by the impurity photovoltaic effect”. *Journal of applied physics*, **75**(8) 4022-4031(1994).

5. G. Azzouzi and W. Tazibt, “Improving Silicon Solar Cell Efficiency by Using the Impurity Photovoltaic Effect”. *Energy Procedia*, **41**, 40-49 (2013).
6. M. A. Green, “Multiple bands and impurity photovoltaic solar cells: General Theory and comparison to tandem cells”. *Prog. Photovolt. Res. Appl.*, **9**, 137–144 (2001).
7. M. C. Beard. “Multiple Exciton generation in semiconductor quantum dots”. *The Journal of Physical Chemistry Letters*, **2**(11), 1282-1288 (2011).
8. R. T. Ross, A. Nozik. “Efficiency of hot carrier solar energy converters”. *Journal of Applied Physics*, **53**(5), 3813-3818 (1982).
9. A. Luque and A. Marti, “Increasing the efficiency of ideal solar cells by photon induced transitions at intermediate levels”. *Physical Review Letters*, **78**(26), 5014 (1997).
10. A. Luque, A. Marti. “The intermediate band solar cell: progress toward the realization of an attractive concept”. *Advanced Materials*, **22**(2), 160-174 (2010).
11. A. Marti, A. Luque, C. Stanley, “Understanding intermediate-band solar cells”. *Nature Photonics*, **6**(3), 146-152 (2012).
12. A. Hadipour, B.de Boer, P. W. Blom. “Organic tandem and multi-junction solar cells”. *Advanced functional materials,* **18**(2), 169-181 (2008).
13. S. K. Shrestha, P. Aliberti and G. J. Conibeer. “Energy selective contacts for hot carrier solar cells”. *Solar Energy Materials and Solar Cells,* **94**(9), 1546-1550 (2010).
14. Y. Takeda, T. Ito, T. Motohiro, D. König, S. Shrestha, G. Conibeer. “Hot carrier solar cells operating under practical conditions”. *Journal of Applied Physics,* **105**(7), 074905 (2009).
15. Y. Takeda, T. Motohiro. “Intermediate band-assisted hot carrier solar cells using indirect bandgap absorbers”. *Progress in Photovoltaics: Research and Applications,* **21**(6), 1308-1318 (2013).
16. W. R. Blevin, W. J. Brown. “A precise measurement of the Stefan-Boltzmann constant”. *Metrologia*, **7**(1), 15 (1971).